



ELSEVIER

Available online at www.sciencedirect.com



AGRICULTURAL
AND
FOREST
METEOROLOGY

Agricultural and Forest Meteorology xxx (2006) xxx–xxx

www.elsevier.com/locate/agrformet

Leaf area index measurements at Fluxnet Canada forest sites

Jing M. Chen^{a,*}, Ajit Govind^a, Oliver Sonnentag^a, Yongqin Zhang^a,
Alan Barr^b, Brian Amiro^c

^a Department of Geography, University of Toronto, 100 St. George Street, Toronto, Ontario, Canada M5S 3G3

^b Meteorological Service of Canada, Environment Canada, Saskatoon, Saskatchewan, Canada S7N 3H5

^c Department of Soil Science, University of Manitoba, Winnipeg, Manitoba, Canada R3T 2N2

Abstract

Leaf area index (LAI) measurements made at 17 forest sites of the Fluxnet Canada Research Network are reported here. In addition to LAI, we also report other major structural parameters including the effective LAI, element clumping index, needle-to-shoot area ratio, and woody-to-total area ratio. Values of the fraction of photosynthetically active radiation (FPAR) absorbed by green leaves in these stands at noon of 15 August are also provided, and a procedure is suggested for using the effective LAI for estimating FPAR at various times of the day and year. Labour-intensive laboratory measurements of the needle-to-shoot area ratio were made for five conifer sites. For each site, 45 shoot samples were measured at three heights from three trees. LAI-2000, TRAC and digital hemispherical photography (DHP) were used in the field, and good agreements between these techniques were obtained. In particular, the low cost DHP technique agreed within 21% of LAI-2000 in terms of effective LAI measurements and 12% of TRAC in terms of element clumping index measurements, suggesting a possibility of using DHP alone for indirect LAI measurements. However, LAI-2000 and TRAC are still found to be more reliable than DHP because of some remaining technical issues with DHP. We confirm the correct method for determining the photographic exposure proposed in previous studies and suggest optimum zenith angle ranges in photograph processing to estimate the effective LAI and the clumping index.

© 2006 Published by Elsevier B.V.

Keywords: LAI; FPAR; TRAC; LAI-2000; Digital hemispherical photography; Clumping; Multiple scattering

1. Introduction

The leaf area index, defined as one half the total green leaf area per unit ground surface area (Chen and Black, 1992a; see also review by Jonckheere et al., 2004), is a basic and indispensable parameter for interpreting carbon, water and energy fluxes measured at tower sites. It is also of interest to modelers who attempt to upscale these tower fluxes to regions based

on biospheric data. The Fluxnet Canada Research Network (FCRN) stresses, in its network design, the importance of acquiring accurate and consistent LAI measurements across the network by forming a special task team to visit all forest sites in the network. The LAI values of all FCRN main forests sites and some satellite sites are reported here.

Through previous works, various LAI indirect measurement techniques have been tested, and theories behind these techniques are becoming mature (Jonckheere et al., 2004; Weiss et al., 2004). These techniques are shown to be comparable with labour-intensive direct (destructive) measurements (Chen et al., 1997; Gower et al., 1999). However, indirect measurements of LAI still

* Corresponding author. Tel.: +1 416 978 7085.

E-mail addresses: chenj@geog.utoronto.ca (J.M. Chen),
Alan.barr@ec.gc.ca (A. Barr), Brian_Amiro@umanitoba.ca (B. Amiro).

face challenges in quantifying foliage clumping at various scales, and in particular, clumping of needles in shoots in conifer stands is one of the main sources of LAI measurement error (Chen et al., 1997). Based on previous film-based hemispherical works (Brown, 1962; Anderson, 1964; Olsson et al., 1982; Chan et al., 1986; Rich, 1990; Chen et al., 1991; Baret et al., 1993; Whitford et al., 1995), digital hemispherical photography (DHP) techniques are becoming increasingly popular (Englund et al., 2000; Frazer et al., 2001; Wagner, 2001; Walter et al., 2003; Leblanc et al., 2005; Zhang et al., in press) as a digital camera system costs less than other instruments and contain much detailed canopy structural information. The gap size analysis theory of Chen and Cihlar (1995) has been applied to hemispherical photographs (Walter et al., 2003; Leblanc et al., 2005) and multi-band canopy images (Kucharik et al., 1999) to address the issue of foliage clumping. There seems to be a potential that a digital camera system can substitute all current LAI instruments including LAI-2000 (Li-Cor, Nebraska, USA) and TRAC (Third Wave Engineering, Ottawa, Canada) for measurements in forest stands. In addition to reporting LAI values and their components in forest sites in Fluxnet Canada, the purpose of this present study is also to investigate several technical issues in LAI measurements including: (i) fast and reliable laboratory measurements of the needle-to-shoot area ratio to quantify within-shoot clumping, and (ii) the reliability of DHP gap fraction analysis to obtain the effective LAI and the reliability of DHP gap size analysis to obtain the clumping information.

2. LAI measurement theory

Through previous theoretical development and validation (Chen, 1996a; Chen et al., 1997), the following governing equation is used for determining LAI (denoted as L):

$$L = \frac{(1 - \alpha)L_e\gamma_E}{\Omega_E} \quad (1)$$

where α is the woody-to-total leaf area ratio, L_e the effective LAI, γ_E the needle-to-shoot area ratio, and Ω_E is the element clumping index. The effective LAI can be accurately measured using the LAI-2000 instrument, or less accurately with a hemispherical photography technique (Zhang et al., in press), based on the Miller (1967) theory (Chen, 1996a):

$$L_e = 2 \int_0^{\pi/2} \ln \left[\frac{1}{P(\theta)} \right] \cos \theta \sin \theta d\theta \quad (2)$$

where $P(\theta)$ is the measured canopy gap fraction at zenith angle θ , which is the best when averaged over the entire azimuthal angle range. Accurate measurement of L_e requires hemispherical $P(\theta)$ data, and both LAI-2000 and hemispherical photography can provide the data through sensing the diffuse radiation from the sky over the hemisphere. While there are issues of the accuracy of hemispherical photography techniques associated with exposure and processing (Chen et al., 1991; Wagner, 2001; Zhang et al., in press), LAI-2000 can provide reliable estimates of L_e , although the multiple scattering effect can cause a considerable underestimation of L_e and should be corrected (Chen, 1996b).

The remaining major challenge in optical LAI measurements lies in getting the other parameters in Eq. (1). The determination of α should theoretically require destructive sampling because green and non-green materials in conifer canopies are not easily separated by optical means, although Kucharik et al. (1997) developed an instrument for this purpose. Even though non-green materials can be differentiated from green materials from an upward-looking camera in multiple spectral bands, the probability of their overlapping would incur considerable uncertainty (Kucharik et al., 1999). In this study, this parameter in conifer stands was not measured, but we rely on estimates based on forest age and hemispherical photographs where the amount of tree trunks is clearly visible. In a broadleaf stand, it was estimated through LAI-2000 measurements before the growing season using the methodology of Barr et al. (2004).

Foliage clumping (Nilson, 1971) is separated into two scales: within-shoot clumping and beyond-shoot clumping (Chen and Cihlar, 1995). This separation is necessary because optical instruments are generally incapable of measuring gaps between needles within a shoot. This level of foliage clumping was recognized and estimated in various ways by Oker-Blom (1986), Gower and Norman (1990), Stenberg et al. (1994), Fassnacht et al. (1994), etc. Based on a theoretical development by Chen (1996a), this clumping is quantified using the needle-to-shoot area ratio (γ_E) as follows:

$$\gamma_E = \frac{A_n}{A_s} \quad (3)$$

where A_n is half the total needle area (including all sides) in a shoot, and A_s is the half the shoot area defined as

$$A_s = \frac{1}{\pi} \int_0^{2\pi} d\phi \int_0^{\pi/2} A_p(\theta, \phi) \cos \theta d\theta \quad (4)$$

where ϕ is the azimuthal angle difference between the direction of light and the main axis of the shoot, θ the zenith angle, and $A_p(\theta, \phi)$ is the projected area of the shoot. If the shoot is spherical, the projected area is the same in all directions, and A_s would be twice A_p , i.e. the hemispherical area is twice the projected area (disk). Procedures in using Eq. (4) in practice are given in Section 3.5.

Beyond-shoot clumping (Ω_E) is quantified using the element clumping index and measured directly in the field using either TRAC or DHP based on a canopy gap size distribution theory (Chen and Cihlar, 1995; Leblanc et al., 2005). This clumping includes the effect of canopy structures larger than shoots, including tree crowns, whorls, branches, etc. It is determined using the following equation (Chen and Cihlar, 1995; Leblanc, 2002):

$$\Omega_E(\theta) = \frac{\ln[F_m(0, \theta)]}{\ln[F_{mr}(0, \theta)]} \frac{[1 - F_{mr}(0, \theta)]}{[1 - F_m(0, \theta)]} \quad (5)$$

where $F_m(0, \theta)$ is the total canopy gap fraction at zenith angle θ , i.e. the accumulated gap fraction from the largest to smallest gaps; and $F_{mr}(0, \theta)$ is the total canopy gap fraction after removing large gaps resulting from the non-random foliage element distribution due to canopy structures such as tree crowns and branches.

3. Sites and experimental methods

3.1. Site description and LAI transects

Most FCRN sites that are measured in this study are described in Courselle et al. (2005), and the description of the eastern white pine sites near the Turkey Lake is found in Peichl and Arain (2006). Therefore, only the main attributes of these sites are provided in Table 1. Also shown in Table 1 are LAI transects established at each flux tower site. At a site, LAI measurements were made along one or two transects of length ranging from 60 to 400 m depending on the homogeneity and size of a

Table 1
Site description and location and LAI transects

Site	Code	Age (2005)	Latitude, longitude	Overstorey	Transect directions (from north)	Transect lengths (m)
Intermediate Douglas Fir, Campbell River, B.C.	IDF	54	49.905, 125.366	<i>Pseudotsuga menziesii</i>	46°, 226°	200, 200
1988 Douglas Fir, Campbell River, B.C.	DF88	14	49.519, 124.902	<i>P. menziesii</i>	46°, 226°	150, 200
Old Mixed Wood, Timmins, Ontario	OMW	74	48.217, 82.156	<i>Picea mariana</i>	270°	400
Eastern Old Black Spruce, Chibougamo, Quebec	EOBS	100	49.692, 74.342	<i>P. mariana</i>	270°, 90°	400, 300
1980 Balsam Fir, Charlie Lake, NB	BF80	25	46.472, 67.100	<i>Abies balsamea</i>	270°	200
Intermediate Balsam Fir, Nashwaak Lake, NB	IBF	38	46.474, 67.098	<i>A. balsamea</i>	270°	300
Young Balsam Fir, Nashwaak Lake, NB	YBF	32	46.477, 67.077	<i>A. balsamea</i>	325°	300
1942 White Pine Plantation, Turkey Lake, Ontario	WPP39	66	42.710, 80.357	<i>Pinus strobus</i>	180°	200
1970 White Pine Plantation, Turkey Lake, Ontario	WPP74	31	42.709, 80.348	<i>P. strobus</i>	180°	200
1985 White Pine Plantation, Turkey Lake, Ontario	WPP89	16	42.773, 80.459	<i>P. strobus</i>	180°	200
1977 Fire Candle Lake, Sask.	F77	28	54.485, 105.817	<i>Pinus banksiana</i>	0°	100
1998 Fire Candle Lake, Sask.	F98	7	53.917, 106.078	<i>P. banksiana</i>	90°	100
Old Aspen, Prince Albert, Sask.	OA	84	53.629, 106.200	<i>Populus tremuloides</i>	225°, 135°	300, 60
Southern Old Black Spruce, Candle Lake, Sask.	SOBS	123	53.987, 105.117	<i>P. mariana</i>	135°, 67°	100, 60
Southern Old Jack Pine, Candle Lake, Sask.	SOJP	88	53.916, 104.690	<i>P. banksiana</i>	135°, 67°	200, 60
1975 Harvested Jack Pine, Candle Lake, Sask.	HJP75	30	53.875, 104.045	<i>P. banksiana</i>	135°, 325°	150, 150
1994 Harvested Jack Pine, Candle Lake, Sask.	HJP94	11	53.908, 104.690	<i>P. banksiana</i>	325°	100

More descriptions are in Coursolle et al. (in press).

176 site. At the mixed hardwood site at Timmins, for
177 example, where the stand is extensive and variable
178 because of the species mixture, the transect was 400 m
179 long, while at the eastern white pine (*Pinus strobus* L.)
180 sites near Turkey Lake, where the stand size is limited
181 but uniform, only 200 m transects were measured. At
182 satellite sites, transects are correspondingly short. The
183 transects generally ran from the flux tower to the
184 prevailing wind direction in order to characterize the
185 portion of the canopy that influences most the measured
186 energy, water and carbon fluxes. At the Douglas-fir
187 (*Pseudotsuga menziesii* (Mirb.) Franco) sites on the
188 Vancouver Island, the transects ran in two directions
189 from the tower: southwest (226° from north) and
190 northeast (46° from north) corresponding to the daytime
191 sea-breeze direction and nighttime Katabatic flow
192 direction, respectively. The directions of transects
193 given in Table 1 are the compass bearing subtracted
194 by the magnetic north (varying between sites), so they
195 are in geographic coordinates.
196

3.2. LAI measurement protocol

197 We followed the LAI measurement protocol of Chen
198 et al. (2002) to estimate all needed parameters in
199 Eq. (1):

- 200 (1) To measure the effective LAI (L_e) at all sites, using
201 LAI-2000 as the main instrument. With new
202 development in measurement techniques, a DHP
203 technique can be used as an alternative when
204 recommended procedures are followed (Zhang
205 et al., *in press*).
- 206 (2) To measure the element clumping index (Ω_E) at all
207 sites, using TRAC as the main instrument. The
208 alternative DHP technique can also be used for this
209 purpose, but generally with less accuracy (Leblanc
210 et al., 2005).
- 211 (3) To measure the needle-to-shoot area ratio (γ_E)
212 where possible. Otherwise suggested default values
213 for various forest types can be used (Chen, 1996a).
214 This current study suggests more values.
- 215 (4) To measure the woody-to-total area ratio (α) where
216 possible. Otherwise they can be estimated based on
217 forest types and age according to previous experi-
218 mental results (Chen, 1996a; Kucharik et al., 1998).
219
220

221 In the present study, we focus on the following issues
222 in the protocol: (i) using DHP for clumping estimation
223 through applying Chen and Cihlar (1995) gap size ana-
224 lysis method, and (ii) reducing errors in LAI estimation
225 by carrying out a large amount of labour-intensive

230 measurements of the needle-to-shoot area ratio. While
231 further research is still needed to measure the woody-to-
232 total area ratio non-destructively, we only use the best
233 estimates on this parameter for the final LAI estimation
234 using Eq. (1). Although this measurement protocol is
235 developed based on our experience with boreal forests,
236 it would be applicable to other ecosystems. We enco-
237 urage other flux networks to carry out LAI measure-
238 ments using consistent techniques and protocols so that
239 flux data can be effectively compared across sites and
240 networks.
241

3.3. LAI-2000 and TRAC measurements

242 Along the transect(s) at each site, forestry marker
243 flags were inserted to the forest floor every 10 m.
244 Generally, two LAI-2000 units were used each time,
245 one mounted on the top of the tower in a continuous
246 logging mode and one used inside the stand at each flag.
247 As different units were used each time, they were
248 synchronized and calibrated following recommended
249 procedures in the LAI-2000 manual. The measurements
250 were made either in the evening when the sun is below
251 75° from the zenith or under an overcast sky. A 90° view
252 cap was used on both units to block any remaining direct
253 light and to avoid the influence of the operator on the
254 sensor. The operator always stood between the sensor
255 and the sun.
256

257 The TRAC was walked on the same transect on clear
258 days, and at each 10 m flag, a distance mark was
259 registered in the data stream by pressing a button. In
260 dense stands where the TRAC sensor did not fully
261 expose to the sun, reference measurements for the direct
262 light above the canopy was made in a large opening or
263 outside the stand. In addition to measuring the element
264 clumping index, TRAC also produces the effective LAI
265 and the LAI after using additional inputs of the needle-
266 to-shoot area ratio and woody-to-total area ratio. In
267 heterogeneous stands, the effective LAI from TRAC
268 could be significantly different from that from LAI-
269 2000 as TRAC measures it only along the sun's
270 direction while LAI-2000 provides the average for the
271 hemisphere. We therefore used the effective LAI from
272 LAI-2000 in our final LAI calculation.

273 Although LAI-2000 provides the average effective
274 LAI for a much larger angular domain than does TRAC,
275 it can suffer from a large error due to multiple scattering
276 of light in the canopy. This is because the instrument
277 assumes that leaves are black in blue wavelengths (400–
278 490 nm) used for canopy gap fraction estimation, but in
279 reality leaves have considerable blue scattering albedos.
280 This multiple scattering effect on LAI retrieval is most

280 significant at the largest zenith angles at which the gap
281 fraction is smallest. A useful way to investigate this
282 multiple scattering effect is to ignore rings 4 and 5 of
283 LAI-2000 data using the available C2000 software,
284 corresponding to the zenith angle ranges from 45° to 60°
285 and 60° to 74°, respectively, to see the impact of these
286 rings on the calculated LAI. The caveat of this approach
287 is the assumption of a spherical leaf angle distribution,
288 i.e. the extinction coefficient being a constant. This
289 assumption may not be valid for conifer canopies,
290 which often have vertical tree crowns and horizontal
291 branches. We will assess the effect of this assumption on
292 LAI estimation in Section 4.
293

294 3.4. Hemispherical photograph acquisition and 295 processing

296 We took the opportunity of network-wide LAI
297 measurements to test the utility of the digital hemi-
298 spherical photography (DHP) technique for LAI mea-
299 surements, based on the recent work by Leblanc et al.
300 (2005). DHP data were acquired at most sites using a
301 Nikon CoolPix 4500 digital camera with a Nikon FC-E8
302 fisheye lens. In order to test the accuracy of DHP for both
303 the effective LAI and the element clumping index estim-
304 ation, the exposure of the photographs followed a strict
305 procedure, based on the recommendation of Zhang et al.
306 (in press). Briefly, the correct exposure for a photograph
307 taken inside a stand was determined universally to be two
308 stops of overexposure relative to the sky reference
309 exposure, i.e. the automatic exposure of the sky deter-
310 mined outside the stand. Since the reference exposure
311 often changed considerably, especially near sunset,
312 between the start and end of measurements along a
313 transect, L_e at a location near the middle of the transect
314 was taken as the weighted mean of L_e values calculated
315 separately with two photographs taken at two exposures
316 referenced to the sky exposure at the beginning and end of
317 the measurements, respectively. We normally took three
318 to five photographs of different exposures at a flag
319 position.

320 Fisheye photographs were processed with the DHP
321 software to derive the effective LAI (Leblanc et al.,
322 2005). Based on two threshold values, the software
323 identifies pixels of pure sky, pure plant, and mixture of
324 these two, and an unmixing method is used to estimate the
325 gap fraction within mixed pixels (Leblanc et al., 2005). A
326 circular photograph was divided into concentric 15 rings
327 spanning the zenith angle range from 0° to 75°. To avoid
328 problems of missing small gaps in DHP at large zenith
329 angles, the effective LAI was calculated using the ring
330 corresponding to zenith angle range of 55–60°, following

331 the recommendation of Leblanc et al. (2005). The
332 clumping index was derived through the combined use of
333 the DHP and TRAC softwares. In DHP, a string of digital
334 numbers along a concentric circle on the photograph,
335 corresponding to a zenith angle, was extracted from each
336 photograph and imported to TRAC software, where this
337 string was treated as a TRAC measurement along a
338 transect and converted it to canopy gaps of various sizes,
339 from which the element clumping index was estimated.
340 The DHP software allows this data string extraction at 1°
341 intervals over the entire zenith angle range from 0° to 75°,
342 and the clumping variation with zenith angle was
343 investigated by Leblanc et al. (2005). Generally, the
344 index increases with zenith angle by about 20% from
345 zenith to 75°. This increase is caused by both structural
346 and optical reasons. Structurally, large gaps disappear at
347 large zenith angles, making the canopy appear less
348 clumped (higher clumping index). Optically, the mea-
349 sured gap size distribution may be distorted at large
350 zenith angles because the image resolution (normally
351 1704 × 2272 pixels) is still not high enough to resolve all
352 small gaps, making the foliage element size considerably
353 larger than the shoot size in conifer stands. In this study,
354 therefore, we computed the element clumping index from
355 DHP within the zenith angle range 40–45°, a compromise
356 of the suggested angle of 57.5° (Leblanc et al., 2005) and
357 measurement accuracy.

358 3.5. Needle-to-shoot area ratio measurement

359 In each forest stand, 45 shoot samples were taken
360 from three trees: one dominant (D), one co-dominant
361 (M) and one suppressed (S), at three heights: top (T),
362 middle (M) and bottom (L), forming nine classes
363 containing five shoot samples each: DT, DM, DL, MT,
364 MM, ML, MS, ST, SM, and SL (e.g., DT means top
365 height of a dominant tree). They were taken from trees
366 either via a canopy access tower or a crane lift. These
367 samples were kept in electrical coolers at a temperature
368 slightly above 0 °C and analyzed within a week in
369 laboratory. A system, consisting of a digital camera
370 (Toshiba PDR-4300) mounted on a firm copy stand
371 (Regent Instruments Inc., Canada), a light table (Kaiser
372 Prolite 5000, Germany), and a Windows-based personal
373 computer with an image analysis software, was used to
374 measure the projected shoot areas. The volume
375 displacement method described in Chen et al. (1997)
376 was used to measure the needle area in a shoot. As no
377 empirical coefficients were available in Chen et al.
378 (1997) for converting the volume to the surface area for
379 needles with elliptical cross sections (Douglas-fir,
380 balsam fir [*Abies balsamea* (L.) Mill.] and of bifurcated

cylinder shapes (eastern white pine), we develop additional empirical equations according to needle thickness (a) to width (b) ratio:

$$A_n = f\sqrt{Vnl} \quad (7)$$

where f is a shape factor for elliptical and bifurcated cylinders separately:

$$f_{\text{elliptical}} = 0.5\sqrt{\pi h \times \left(1 + \frac{1}{h}\right)}, \quad h = \frac{a}{b} \quad (8)$$

and

$$f_{\text{b-cylinder}} = \sqrt{\frac{n}{\pi}} + \sqrt{\frac{\pi}{n}} \quad (9)$$

where n is the number of bifurcations. For eastern white pine, $n = 5$.

The calculation of the half the total shoot area needed for estimating the needle-to-shoot area ratio is based on Eq. (4). As many shoot samples were analyzed, we took the approach of Chen (1996a) to measure the projected shoot area at only three camera incidence angles: 0° , 45° and 90° relative to the shoot main axis at one azimuth angle of 0° , i.e. obtaining $A_p(0^\circ, 0^\circ)$, $A_p(45^\circ, 0^\circ)$, and $A_p(90^\circ, 0^\circ)$. The following equation was used to calculate half the total shoot area:

$$A_s = 2 \frac{A_p(0^\circ, 0^\circ) \cos(15^\circ) + A_p(45^\circ, 0^\circ) \cos(45^\circ) + A_p(90^\circ, 0^\circ) \cos(75^\circ)}{\cos(15^\circ) + \cos(45^\circ) + \cos(75^\circ)} \quad (10)$$

This is Eq. (4) simplified for three angle measurements. Chen (1996a) compared this simple three-angle method with 21- and 39-angle projection methods, the difference was within 2% in three stands and 5% in one stand,

suggesting this simple three-angle method is accurate for our purpose.

4. Results

4.1. Needle-to-shoot area ratio

The values of the measured needle-to-shoot area ratio for five stands are summarized in Table 2. The mean value for the mature Douglas-fir stand is 1.66, in reasonable agreement with the value of 1.77 reported in Chen and Black (1992b) for the same species using only several shoot samples. The value of 1.61 for the young Douglas-fir stand is only slightly smaller than that for the mature stand. The mean values for a balsam fir stand in New Brunswick and a white pine stand in southern Ontario are 1.71 and 1.91, respectively. Both values are considerably larger than the mean value of 1.41 reported by Chen (1996a) for six black spruce (*Picea mariana* (Mill.) B.S.P.) and jack pine (*Pinus banksiana* Lamb.) stands in Saskatchewan and Manitoba. The value of 1.57 for a black spruce stand in Quebec is the intermediate case. It appears that the needle-to-shoot area ratio is mostly determined by the growth conditions. In areas with better growing conditions, needles in shoots are denser, making larger needle-to-shoot area ratios. The variations of this ratio among the nine classes of shoot samples show similar patterns as those found by Chen (1996a): (i) dominant trees generally have the largest values, followed by co-dominant and suppressed trees; (ii) shoots at higher levels generally have larger values. These systematic variation patterns and considerable differences among classes suggest that this shoot stratification strategy is necessary for obtaining a reliable mean value for a stand, and the accuracy can still increase if more shoot samples are analyzed.

Table 2
Needle-to-shoot area ratio (γ) of some of the coniferous species in Canada

	IDF	DF88	YBF	WPP39	EOBS
DT	2.00 ± 0.17	1.20 ± 0.04	2.29 ± 0.46	2.00 ± 0.24	1.70 ± 0.28
DM	1.67 ± 0.09	1.47 ± 0.14	1.73 ± 0.13	1.96 ± 0.14	1.51 ± 0.29
DL	1.15 ± 0.10	1.24 ± 0.07	1.40 ± 0.05	1.83 ± 0.26	1.28 ± 0.10
MT	1.66 ± 0.25	1.74 ± 0.12	1.83 ± 0.23	2.05 ± 0.16	1.60 ± 0.22
MM	1.59 ± 0.17	1.63 ± 0.12	1.85 ± 0.13	1.75 ± 0.23	1.64 ± 0.27
ML	1.65 ± 0.08	1.66 ± 0.52	1.34 ± 0.20	1.77 ± 0.14	1.66 ± 0.19
ST	1.61 ± 0.21	1.94 ± 0.09	1.87 ± 0.23	2.02 ± 0.20	1.67 ± 0.18
SM	1.57 ± 0.14	2.01 ± 0.26	1.65 ± 0.15	2.00 ± 0.11	–
SL	2.02 ± 0.12	1.57 ± 0.35	1.44 ± 0.05	1.85 ± 0.16	1.47 ± 0.13
Mean	1.66 ± 0.15	1.61 ± 0.19	1.71 ± 0.18	1.91 ± 0.18	1.57 ± 0.14

In each forest stand, 45 shoot samples were taken from three trees: one dominant (D), one co-dominant (M) and one suppressed (S), at three heights: top (T), middle (M) and bottom (L), forming nine classes with five shoot samples each: DT, DM, DL, MT, MM, ML, MS, ST, SM, and SL.

Table 3
Mean LAI values in forest sites in Fluxnet Canada Research Network, measured in 2003–2005

Site code	L_e LAI-2000		L_e TRAC	L_e DHP 55–60°	Green FPAR at noon 15 August	α	γ_E	Ω_E DHP 40–45°	Ω_E TRAC	LAI DHP	LAI TRAC	LAI LAI-2000+ TRAC _A
	1–3 ^a	1–5										
IDF	4.34	3.83	3.38	3.57	0.79	0.20	1.66	0.91	0.81	5.9	5.6	7.3
DF88	2.83	2.50	–	2.50	0.69	0.10	1.61	0.89	–	4.7	–	4.7^b
OMW	3.90	3.53	–	3.69	0.78	0.15	1.15	0.93	–	4.5	–	4.3^b
EOBS	2.65	2.11	2.22	1.68	0.62	0.15	1.57	0.88	0.92	3.0	3.3	3.7
BF80	6.47	5.37	5.65	4.35	0.87	0.15	1.71	0.95	0.96	7.7	8.5	9.4
IBF	6.28	5.11	5.75	4.90	0.86	0.20	1.71	0.95	0.96	8.2	8.7	8.4
YBF	6.24	5.13	5.19	5.07	0.86	0.20	1.71	0.96	0.94	8.4	7.5	8.6
WPP39	5.55	4.42	5.22	4.01	0.81	0.20	1.91	0.94	0.98	7.6	8.2	8.0
WP74	3.37	3.30	3.82	–	0.72	0.20	1.91	–	0.99	–	5.9	5.9
WPP89	7.11	6.77	6.23	–	0.91	0.15	1.91	–	1.0	–	10.2	12.8
F77	–	–	2.82	–	0.69	0.15	1.40	–	0.99	–	3.4	–
F98	–	–	1.31	–	0.34	0.40	1.40	–	0.97	–	1.1	–
OA	–	1.90	2.44	–	0.55	0.15	1.00	–	0.87	–	2.4	2.1
SOBS	–	2.57	2.72	–	0.65	0.15	1.36	–	0.90	–	3.5	3.8
SOJP	–	1.68	1.76	–	0.49	0.20	1.42	–	0.85	–	2.5	2.6
HJP75	–	1.86	2.07	–	0.54	0.15	1.44	–	0.93	–	3.1	2.9
HJP94	–	–	0.48	–	0.22	–	1.44	–	0.83	–	0.8	–

Also shown are all parameters needed to calculate LAI using Eq. (1). Three techniques are used: LAI-2000, TRAC and digital hemispherical photography (DHP). The combination of LAI-2000 and TRAC provides the best estimates (in **bold**). In the final LAI calculations, L_e values from LAI-2000 (rings 1–5) are increased by 16% to account for multiple scattering effect (see Section 4.2).

^a Rings 4 and 5 in LAI-2000 data are blocked in processing.

^b Ω_E from DHP is used in the absence of TRAC data.

4.2. Leaf area index

All parameters required for LAI estimation using Eq. (1) are summarized in Table 3. The final LAI values are given on three separate columns: (i) from the combination of TRAC (for clumping) and LAI-2000 (for L_e), which is in bold to indicate that this column gives the best estimates; (ii) from TRAC only; (iii) from DHP only. TRAC is capable of measuring both L_e and clumping, but in extensive stands, L_e measured at one or several zenith angles is less reliable as the stand average than that of LAI-2000 which is based on hemispherical measurements. However, the difference in LAI estimation with the added L_e information from LAI-2000 is found to be only mildly significant based on the comparison of the best estimates and the TRAC estimates (Fig. 1). Therefore, walking TRAC over a transect at a few zenith angles can generally obtain LAI values within 10% of the best estimate, and only in two cases, IDF and WP85, TRAC values are 23% and 26% smaller than the best estimates, respectively. At the IDF site, TRAC measurements were made in October 2005, while LAI-2000 measurements were made in August 2004, and the variations between years and between seasons might have contributed significantly to the differences between TRAC and the best estimate. At the WP85 site, the forest was very dense with little penetration of either direct or diffuse light, and

the LAI measurements from all instruments were prone to error because the inverted LAI using the Beer's Law becomes highly sensitive to small errors in the radiation transmission measurements at high LAI values. However, there is little doubt that the LAI of the WP85 stand was larger than 10. For the OA site, the LAI is the mean of 3.1, 2.5, and 2.6 for 2003, 2004, and 2005, respectively, in the mid-summer for the overstorey only. The understorey LAI was generally as large as the overstorey, and the total LAI varied in the range from 3.7 to 5.2 in the period of 1994–2003 (Barr et al., 2004).

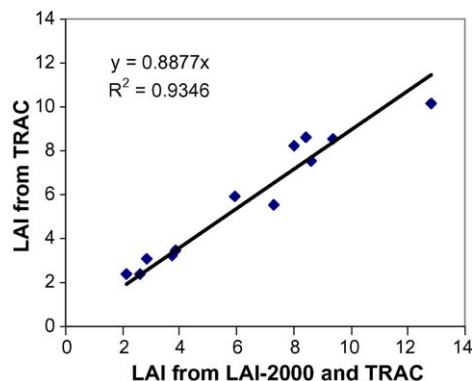


Fig. 1. Comparison of LAI values derived from TRAC with those derived from combining LAI-2000 for the effective LAI and TRAC for element clumping.

476
477 For most stands, LAI-2000 data were processed for L_e
478 in two ways: (i) using all five rings, and (ii) using only
479 rings 1–3, for the purpose of studying the multiple
480 scattering effect (see Section 3.3 for reasons). It is inter-
481 esting to note that L_e based on rings 1–3 is consistently
482 larger than that based on rings 1–5, indicating indeed that
483 stronger multiple scattering effects existed at larger
484 zenith angles. The average difference between these two
485 ways of L_e calculation is 16%. If the leaf angle
486 distribution is spherical, the difference between these
487 two cases in each stand can be entirely attributed to the
488 multiple scattering effect. However, conifer canopies are
489 complex with horizontal branches and vertical tree
490 crowns, and the effective leaf angle distribution can
491 deviate from the spherical distribution to a considerable
492 extent. For Douglas-fir canopies with distinct horizontal
493 branches, causing the extinction coefficient to decrease
494 with zenith angle (Chen and Black, 1991), the L_e
495 measured in near the vertical direction is larger than that
496 in near the horizontal direction, and the difference in L_e
497 between these two angle ranges (1–3 and 1–5 rings) may
498 be partly offset by this structural effect, i.e. the difference
499 is smaller than the scattering effect alone. For black
500 spruce, where the vertical crown structures are more
501 apparent than the short horizontal branches, making the
502 extinction coefficient increase with zenith angle (Chen,
503 1996b), the difference may be larger than the multiple
504 scattering effect alone. In terms of angular canopy
505 structure, balsam fir and eastern white pine may be the
506 intermediate cases between Douglas-fir and black spruce.
507 As these angular structural effects on the difference in L_e
508 estimated in the two zenith angle ranges differ in different
509 stands, some positive and some negative, we estimate the
510 multiple scattering effect by simply taking the arithmetic
511 mean of the ratio of the L_e value calculated in rings 1–3 to
512 that calculated in rings 1–5, with the assumption that
513 structural effects average out in stands of contrasting
514 angular structures. The average ratio is 1.16, meaning
515 that the multiple scattering effect caused a negative bias
516 of 16% in L_e in these stands. We have therefore increased
517 all L_e values from LAI-2000 and DHP (except those from
518 TRAC) by 16% in the final calculation of LAI (the listed
519 L_e values are not corrected using this ratio).

520 If TRAC could be used to obtain the same spatial and
521 angular averages as the LAI-2000, it would be the
522 ultimate way to find this light scattering effect on L_e , but
523 in reality this is difficult to achieve because TRAC only
524 measures in sun's azimuthal direction. In Table 3, the L_e
525 values from TRAC are generally larger than those from
526 LAI-2000 including five rings, also indicating the same
527 light scattering effect. However, in two stands (IDF and
528 WP85), the TRAC values are even smaller than LAI-

2000 values for reasons given in the first paragraph of
this section. Through comparing L_e from TRAC
measurements made at 5–13 zenith angles with those
from LAI-2000 based on rings 1–5, Chen (1996b) found
that the multiple scattering effect was in the range from
0% to 25% for six conifer stands with a mean of 15%, in
good agreement with the value of 16% found in this
study through LAI-2000 ring masking.

The woody-to-total area ratio (α) is estimated based
on visual examination of woody (stem and branch) areas
appearing in photographs and previous values measured
or estimated by Chen (1996a) for stands in Saskatch-
ewan. For the OA site, it was obtained through LAI-
2000 measurements before the growing season (Barr
et al., 2004). For conifer sites, these estimates may be
most uncertain among all parameters in Table 3. At the
F98 site where many dead trees are still standing after
the fire in 1998, the α value is estimated to be 40%. The
needle-to-shoot area ratio (γ) is mostly based on new
measurements made in this study. For stands in
Saskatchewan, values previously measured by Chen
(1996a) are used. For the mixed wood stand near
Timmins, the value of 1.15 was derived as the weighted
average between broadleaf trees ($\gamma = 1.0$) and conifer
trees ($\gamma = 1.57$, taken as the value of EOBS stand in
Quebec). The weights between these two types of trees
were obtained through basal area measurements using a
prism along the transect.

The accuracy of the best estimates of LAI is
conservatively estimated to be 75%, or the total error is
25%, including 10% error in woody-to-total area ratio,
5% error in effective LAI, 5% in needle-to-shoot error
ratio, and 5% in element clumping index. In black
spruce stands, where the top portion of tree crowns is
very dense, there could be an additional 10% under-
estimation of LAI (Chen et al., 1997).

4.3. Reliability of digital hemispherical photography (DHP)

The reliability of the DHP technique may be examined
in two ways: (i) its ability to acquire reliable L_e values,
and (ii) its ability to measure the element clumping index.
First, we carried out point-by-point comparison of L_e
measurements by both DHP and LAI-2000 for all avail-
able points from all sites (Fig. 2). In field measurements,
we took LAI-2000 data every 10 m, while photographs
were generally taken every 50 m because it was more
time consuming. It is encouraging to see that overall DHP
agreed very well with LAI-2000 in terms of L_e . As the
stand average, the largest difference is 21% at the EOBS
site (Table 3). The agreement could have been better if the

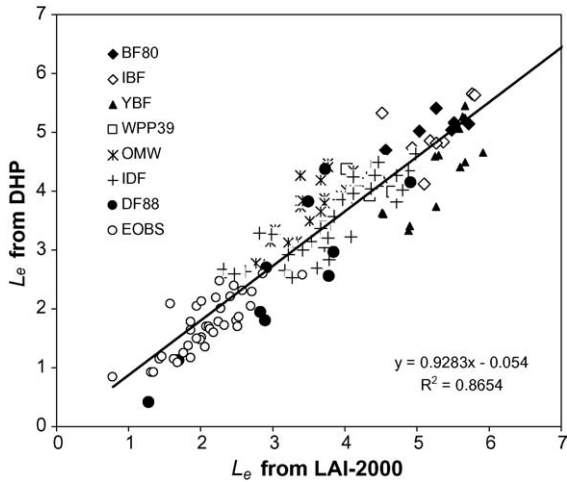


Fig. 2. Comparison of effective LAI (L_e) values measured using the digital hemispherical photography (DHP) technique with those measured using LAI-2000.

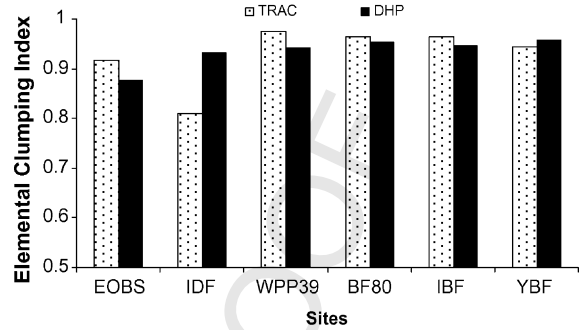


Fig. 3. Comparison of the element clumping index measured using the digital hemispherical photography (DHP) technique with those measured using TRAC.

578
 579 angular exposure and the spatial positions of these two
 580 sensors at each flag position were exactly same, but in
 581 practice, a 90° view cap was used for LAI-2000 while
 582 photographs were exposed to all azimuthal directions,
 583 and for the convenience of operation, the DHP camera
 584 was normally mounted at 1 m above the ground while
 585 LAI-2000 was put at about 0.5 m above the ground. This
 586 good agreement between these two techniques is found
 587 because (i) LAI-2000 was reliable when operated
 588 properly (see Section 3.3) and (ii) strict procedures were
 589 followed for DHP exposure setting and image processing
 590 (see Section 3.4). We emphasize that the DHP exposure
 591 setting is critical for correct determination of L_e . If the
 592 automatic exposure inside the stand was used (as done in
 593 many other studies), the L_e from DHP would have been
 594 underestimated by over 40% in comparison with LAI-
 595 2000 (Zhang et al., *in press*). The automatic exposure
 596 causes this underestimation because it overexposes the
 597 canopy to obtain the mean grey level of 18% while our
 598 purpose is to make the canopy black and sky white. The
 599 correct exposure is two-stops overexposure relative to the
 600 automatic sky exposure determined outside the stand in
 601 order to make sky appear white. The automatic exposure
 602 determined inside the stand is normally one to four stops
 603 more exposure (either longer time or larger aperture) than
 604 the correct exposure depending on the LAI of the stand.
 605 In denser stands, the difference in these two exposure
 606 settings is larger, causing larger underestimation in L_e .
 607 The element clumping index determined from DHP
 608 compared reasonably well with TRAC measurements
 609 (Fig. 3). We averaged the clumping index values from
 610 all correctly exposed photographs taken in each stand to

610
 611 compare with the mean value from TRAC, in order to
 612 minimize the problem of different samplings of these
 613 techniques (TRAC samples a straight line in space,
 614 while DHP samples a circle in the canopy). Overall,
 615 DHP obtains values of the clumping index within 4% of
 616 the TRAC value with the exception at the IDF site,
 617 where the DHP value is larger than the TRAC value by
 618 12%. This again could have been caused by the different
 619 dates of measurements of these two sensors. TRAC was
 620 used a year later than DHP and near the end of the
 621 growing season, and there could be some differences in
 622 the canopy between these 2 years and between seasons.
 623 We do not find this comparison of these two techniques
 624 to be assertive in terms of DHP's ability to determine
 625 clumping. Visual examination of DHP photographs
 626 does reveal much detailed canopy structural informa-
 627 tion, and clumping can indeed be derived from DHP.
 628 However, two nontrivial technical issues still remain: (i)
 629 because of the multiple scattering effect, a significant
 630 fraction of leaves near the vertical direction are lost
 631 even the exposure is correctly determined, and this is
 632 balanced by underexposing the canopy in near the
 633 horizontal direction (to get correct L_e), causing losses of
 634 small gaps at large zenith angles. So a compromise of
 635 using the zenith angles of 40–45° in determining the
 636 clumping value was made in this study; (ii) because of
 637 the loss of small gaps, the gap size distribution is
 638 distorted, and this distortion increases with zenith angle.
 639 We used the method of Chen and Black (1992b) to
 640 determine the projected element width from the gap size
 641 distribution curve (tangent of the log curve at zero gap
 642 size) and found that the width determined in this way
 643 was much larger than the characteristic width of shoots
 644 in the canopy (up to 10 times) and was increasing with
 645 zenith angle, suggesting that as the zenith angle
 646 increased, the ability of DHP to differentiate shoots
 647 decreased. These two issues may be inherent problems

with the DHP technique, and we therefore suggest that we are not yet ready to replace existing optical instruments with DHP for LAI measurements, especially when high accuracy is required. However, DHP techniques can be used for fast and reasonably accurate (75–85%) measurements of LAI by determining the correct exposure in the field and by selecting correct zenith angle ranges in photograph processing: 55–60° for L_e and 40–45° for clumping.

4.4. Fraction of photosynthetically active radiation (FPAR) absorbed by the canopy

FPAR is a parameter needed in light use efficiency models, although these models suffer from serious inaccuracy in photosynthesis estimation because of their inability to differentiate diffuse and direct light effects (Chen et al., 2003). FPAR was measured accurately using TRAC because the technique of walking and high frequency sampling of the transmitted and reflected PAR is the most reliable way to obtain the spatial averages of these PAR components in forest canopies, but the measurements were made in a limited number of sun angles in each stand. However, we should note that FPAR is not an inherent canopy parameter. For the same canopy, FPAR changes greatly with solar zenith angle, and therefore it is diurnally and seasonally variable. For convenience of potential users, we provide FAPR values at the solar noon of 15 August for all stands in Table 3. They are calculated using the unmasked LAI-2000 L_e data in Table 3 (after making the 16% correction, see Section 4.2). L_e from LAI-2000 rather than from TRAC is used for FPAR estimation because LAI-2000 provides better spatial and angular averages than TRAC. For conifer stands, L_e is almost constant throughout the year (Chen, 1996b), and it can be used to calculate FPAR for any given time on the day and in any season. The following equation (Chen, 1996b) can be used for this purpose:

$$FPAR = (1 - \rho_a) - (1 - \rho_u) e^{-0.45(1-\alpha)L_e/\cos\theta} \quad (11)$$

where ρ_a is the PAR albedo above the canopy, and ρ_u is the PAR albedo of the forest floor. They were found to be 0.05 and 0.06 for conifer stands, respectively (Chen, 1996b). For simplicity, a constant of 0.45 is given as the extinction coefficient for the global PAR in consideration of the multiple scattering effect on enhancing the PAR transmission, and the L_e values in Table 3 should be multiplied by a factor 1.16 before using Eq. (11). The woody fraction (α) is discounted from L_e in order to obtain FPAR for green leaves only. Given the L_e value, it

is critical to know the solar zenith angle θ . As θ is larger in winter than in summer, the FPAR is also larger in winter (counter intuitive).

5. Conclusions

Through a large team effort, we report LAI values and their components for all major forest sites in Fluxnet Canada Research Network. The accuracy of the final LAI values is estimated to be generally higher than 75% except for black spruce stands which may have an additional 10% underestimation because of extremely dense crown tops. The largest improvements made in this study are the systematic and labour-intensive laboratory measurements of the needle-to-shoot area ratio for five conifer stands. This ratio quantifies a level of foliage clumping that could not be measured in the field. The largest uncertainty in the reported LAI values exists in the estimation of the effect of non-green materials on the indirect measurements of the green leaf area index. This may be a direction to improve in the near future.

Three instruments are compared, including LAI-2000, TRAC and digital hemispherical photography (DHP). Measurements are the best made with the combined use of LAI-2000 for the effective LAI based on hemispherical diffuse radiation transmission and TRAC for the element clumping index based on direct radiation transmission. The DHP technique is shown here to be capable of obtaining similar (within 25% maximum) measurements as those from combining LAI-2000 and TRAC, when the DHP was used following strict procedures of photograph exposure and processing. However, LAI-2000 and TRAC are still considered to be more reliable than DHP because of some remaining inherent technical issues with the DHP technique. These issues may add an error of up to 25% in addition to LAI-2000 and TRAC errors.

Uncited reference

~~Leblanc and Chen (2001).~~

Acknowledgements

This work was supported by the Fluxnet Canada Research Network funded by the Natural Science and Engineering Council of Canada, the Canadian Foundation of Climate and Atmospheric Sciences, and BIO-CAP Canada. Gang Mo of University of Toronto assisted in part of the field measurements. We gratefully acknowledge the logistic support from various people during the field experiments: Zhisheng Xing, Charles

741 Bourque, and Edwin Swift at the New Brunswick sites;
742 Andre Beaudoin, Luc Guindon and Pierre Bernier for
743 the Chibogamou site in Quebec; Harry McCaughey at
744 the Timmins site in Ontario; Altaf Arain at the Turkey
745 Lake sites in Ontario; and Andy Black at the Campbell
746 River sites in B.C. Alison Sass and Natasha Neumann
747 provided assistance in LAI measurements in the various
748 sites in Saskatchewan. Nick Grant did TRAC measure-
749 ments at one of the Campbell River sites.
750

References

- 751 Anderson, M.C., 1964. Studies of woodland light climate. Part 1.
752 The photographic computation of light conditions. *J. Ecol.* 52,
753 27–41.
754 Baret, F., Andrieu, B., Folmer, J.C., Hanocq, J.F., Sarrouy, C., 1993.
755 Gap fraction measurement using hemispherical infrared photo-
756 graphs and its use to evaluate PAR interception efficiency. In: *Varlet-Grancher, C., Bonhomme, R., Sinoquet, H. (Eds.), Crop*
757 *Structure and Light Microclimate: Characterization and Applica-*
758 *tions.* INRA, Paris, pp. 359–372.
759 Barr, A.G., Black, T.A., Hogg, E.H., Kljun, N., Morgenstern, K.,
760 Nestic, Z., 2004. Inter-annual variability of leaf area index of
761 boreal aspen-hazelnut forest in relation to net ecosystem produc-
762 tion. *Agric. For. Meteorol.* 126, 237–255.
763 Brown, H.E., 1962. The canopy camera. *US For. Ser. Rocky Mount*
764 *For. Ecol. Manage.* 11, 139–144.
765 Chan, S.S., McCreight, R.W., Walslad, J.D., Spies, T.A., 1986.
766 Evaluating forest cover with computerized analysis of fisheye
767 photographs. *For. Sci.* 32, 1085–1091.
768 Chen, J.M., 1996a. Optically-based methods for measuring seasonal
769 variation in leaf area index of boreal conifer forests. *Agric. For.*
770 *Meteorol.* 80, 135–163.
771 Chen, J.M., 1996b. Canopy architecture and remote sensing of the
772 fraction of photosynthetically active radiation absorbed by boreal
773 conifer forests. *IEEE Trans. Geosci. Remote Sens.* 34, 1353–1368.
774 Chen, J.M., Black, T.A., 1991. Measuring leaf area index of plant
775 canopies with branch architecture. *Agric. For. Meteorol.* 57, 1–12.
776 Chen, J.M., Black, T.A., 1992a. Defining leaf area index for non-flat
777 leaves. *Plant Cell Environ.* 15, 421–429.
778 Chen, J.M., Black, T.A., 1992b. Foliage area and architecture of
779 clumped plant canopies from sunfleck size distributions. *Agric.*
780 *For. Meteorol.* 60, 249–266.
781 Chen, J.M., Black, T.A., Adams, R.S., 1991. Evaluation of hemi-
782 spherical photography for determining plant area index and geo-
783 metry of a forest stand. *Agric. For. Meteorol.* 56, 129–143.
784 Chen, J.M., Cihlar, J., 1995. Plant canopy gap-size analysis theory for
785 improving optical measurements of leaf area index. *Appl. Opt.* 34
786 (27), 6211–6222.
787 Chen, J.M., Rich, P.M., Gower, S.T., Norman, J.M., Plummer, S.,
788 1997. Leaf area index of boreal forests: theory, techniques, and
789 measurements. *J. Geophys. Res.* 102 (D24), 29429–29443.
790 Chen, J.M., Pavlic, G., Brown, L., Cihlar, J., Leblanc, S.G., White,
791 H.P., Hall, R.J., Peddle, D., King, D.J., Trofymow, J.A., Swift, E.,
792 Van der Sanden, J., Pellikka, P., 2002. Derivation and validation of
793 Canada-wide coarse resolution leaf area index maps using high-
794 resolution satellite imagery and ground measurements. *Remote*
795 *Sens. Environ.* 80, 165–184.
796 Chen, J.M., Liu, L., Leblanc, S.G., Lacaze, R., Roujean, J.L., 2003.
797 Multi-angular optical remote sensing for assessing vegetation
798 structure and carbon absorption. *Remote Sens. Environ.* 84,
799 516–525.
800 Coursolle, C., Margolis, H.A., Barr, A.G., Black, T.A., Amiro, B.D.,
801 McCaughey, J.H., Flanagan, L.B., Lafleur, P.M., Roulet, N.T.,
802 Bourque, C.P.-A., Arain, M.A., Wofsy, S.C., Dunn, A., Morgen-
803 stern, K., Orchansky, A.L., Bernier, P.Y., Chen, J.M., Kidston, J.,
804 Saigusa, N., Hedstrom, N., (in press). Late-summer carbon fluxes
805 from Canadian forests and peatlands along an east-west conti-
806 nental transect. *Can. J. For. Res.*
807 Englund, S.R., O'Brien, J.J., Clark, D.B., 2000. Evaluation of digital
808 and film hemispherical photography and spherical densiometry for
809 measuring forest light environments. *Can. J. For. Res.* 30, 1999–
810 2005.
811 Fasnacht, K., Gower, S.T., Norman, J.M., McMurtrie, R.E., 1994.
812 A comparison of optical and direct methods for estimating
813 foliage surface area index in forests. *Agric. For. Meteorol.*
814 71, 183–207.
815 Frazer, G.W., Fournier, R.A., Trofymow, J.A., Hall, J.R., 2001. A
816 comparison of digital and film fisheye photography for analysis of
817 forest canopy structure and gap light transmission. *Agric. For.*
818 *Meteorol.* 109, 249–263.
819 Gower, S.T., Norman, J.M., 1990. Rapid estimation of leaf area index
820 in forests using the LI-COR LAI-2000. *Ecology* 72, 1896–1900.
821 Gower, S.T., Kucharik, C.J., Norman, J.M., 1999. Direct and indirect
822 estimation of leaf area index, fAPAR, and net primary production
823 of terrestrial ecosystems. *Remote Sens. Environ.* 70, 29–51.
824 Jonckheere, I., Fleck, S., Nackaerts, K., Muys, B., Coppin, P., Weiss,
825 M., Baret, F., 2004. Methods for leaf area index determination.
826 Part I. Theories, techniques and instruments. *Agric. For. Meteorol.*
827 121, 19–35.
828 Kucharik, C.J., Norman, J.M., Murdock, L.M., Gower, S.T., 1997.
829 Characterizing canopy non-randomness with a multiband vegeta-
830 tion imager (MVI). *J. Geophys. Res.* 102 (D24), 29455–29473.
831 Kucharik, C.J., Norman, J.M., Gower, S.T., 1998. Measurements of
832 branch area and adjusting leaf area index indirect measurements.
833 *Agric. For. Meteorol.* 91, 69–88.
834 Kucharik, C.J., Norman, J.M., Gower, S.T., 1999. Characterization of
835 radiation regimes in nonrandom forest canopies: theory, measure-
836 ments, and a simplified modeling approach. *Tree Physiol.* 19, 695–
837 706.
838 Leblanc, S.G., 2002. Correction to the plant canopy gap size analysis
839 theory used by the tracing radiation and architecture of canopies
840 (TRAC) instrument. *Appl. Opt.* 31 (36), 7667–7670.
841 ~~Leblanc, S.G., Chen, J.M., 2001. A practical method for correcting~~
842 ~~multiple scattering effects on optical measurements of leaf area~~
843 ~~index. *Agric. For. Meteorol.* 110, 125–139.~~
844 Leblanc, S.G., Chen, J.M., Fernandes, R., Deering, D.W., Conley, A.,
845 2005. Methodology comparison for canopy structure parameters
846 extraction from digital hemispherical photography in boreal for-
847 ests. *Agric. For. Meteorol.* 129, 187–207.
848 Miller, J.B., 1967. A formula for average foliage density. *Aust. J. Bot.*
849 15, 141–144.
850 Nilson, T., 1971. A theoretical analysis of the frequency of gaps in
851 plant stands. *Agric. Meteorol.* 8, 25–38.
852 Olsson, L., Carlsson, K., Grip, H., Perttu, K., 1982. Evaluation of
853 forest-canopy photographs with diode-array scanner OSIRIS. *Can.*
854 *J. For. Res.* 12, 822–828.
855 Oker-Blom, P., 1986. Photosynthetic radiation regime and canopy
856 structure in modeled forest stands. *Acta For. Fenn.* 197, 1–44.
857 Peichl, M., Arain, M.A., (submitted for publication). Above- and
858 belowground ecosystem biomass and carbon pools in an age-
859 sequence of planted white pine forests. *Agric. For. Meteorol.*
860 861

- 862 Rich, P., 1990. Characterising plant canopies with hemispherical
863 photographs. *Remote Sens. Rev.* 5 (1), 13–29. 873
- 864 Stenberg, P., Linder, S., Smolander, H., Flower-Ellis, J., 1994. Per- 874
865 formance of the LAI-2000 plant canopy analyzer in estimating leaf 875
866 area index of some Scots pine stands. *Tree Physiol.* 14, 981–995. 876
- 867 Wagner, S., 2001. Relative radiance measurements and zenith angle 877
868 dependent segmentation in hemispherical photography. *Agric. 878*
869 For. Meteorol. 107, 103–115. 879
- 870 Walter, J.-M., Fournier, R.A., Soudani, K., Meyer, E., 2003. Integrat- 880
871 ing clumping effects in forest canopy structure: an assessment 881
872 through hemispherical photographs. *Can. J. Remote Sens.* 29 (3), 882
873 388–410. 883
- Weiss, M., Baret, F., Smith, G.J., Jonckheere, I., Coppin, P., 2004. 884
Review of methods for in situ leaf area index (LAI) determination. 875
Part II. Estimation of LAI, errors and sampling. *Agric. For. 876*
Meteorol. 121, 37–53. 877
- Whitford, K.R., Colquhoun, I.J., Lang, A.R.G., Harper, B.M., 1995. 878
Measuring leaf area index in a sparse eucalypt forest: a compar- 879
ison of estimate from direct measurement, hemispherical photo- 880
graphy, sunlight transmittance, and allometric regression. *Agric. 881*
For. Meteorol. 74, 237–249. 882
- Zhang, Y., Chen, J.M., Miller, J., (in press). Determining exposure of 883
digital hemispherical photographs for leaf area index estimation. 884
Agric. For. Meteorol. 885

UNCORRECTED PROOF